**Citation (APA)**
Güneri, R., Petrov, N., Vaucher, C. S., & Yarovoy, A. (2025). A 2D-Localization Approach Based On Block-FOCUSS. In *Proceedings of the 2025 26th International Radar Symposium (IRS)* IEEE.
https://doi.org/10.23919/IRS64527.2025.11046180

# A 2D-Localization Approach Based On Block-FOCUSS

**Rutkay Güneri*, Nikita Petrov*#, Cicero S. Vaucher*#, Alexander Yarovoy***

*Delft University of Technology
Delft, THE NETHERLANDS
email: {r.guneri, n.petrov, c.silveiravaucher, a.yarovoy}@tudelft.nl

#NXP Semiconductors
Eindhoven, THE NETHERLANDS

***Abstract:*** *The problem of enhancing angular resolution capability using a non-coherent radar network has been considered. A 2D-Localization approach based on block-FOCUSS is proposed to overcome the near-field effects. In this method, range-angle coupling due to the large baseline between radar units is taken into account. The performance of the proposed method is compared with two state-of-the-art direction-of-arrival estimation methods which are based on block-FOCUSS and block-OMP.*

## 1. Introduction

Different sensors including camera, lidar, and radar are employed for autonomous driving. Among them, radar offers many advantages like robust performance under adverse weather conditions such as rain, snow, and fog [1]. In addition to all weather operation, radar provides high-resolution range and velocity measurements. However, its main drawback is low angular resolution due to limited aperture size constrained by automotive design requirements. As modern vehicles equipped with multiple radars for advanced driver assistance systems, enhancing radar resolution via a radar network with a distributed aperture [2] might be a solution.

Radar networks are operated coherently or non-coherently. With special hardware and signal processing techniques, coherency between radar units might be established [3]. On the other hand, non-coherent operation reduces the complexity of the system. Different techniques have been proposed to increase angular resolution of non-coherent radar networks. Trilateration [4] and integration of MIMO-DBS images from different radar units [5] are two examples of these methods.

The total aperture of a radar network is composed of the apertures of each radar unit and the baseline between them. An increased aperture size improves the angular resolution of the radar network. However, far-field assumption for target location is violated for the total aperture, although it holds for individual small apertures. Therefore, near-field effects and range-angle coupling [6] should be considered when direction of arrival is estimated with a radar network. The first effect is that the same target will be observed from different aspect angles by different radar units. It causes variations in both angle of arrival and scattering parameters. Secondly,


ISBN 978-3-00-079305-9 

plane wave assumption does not hold for the total aperture of the system. Therefore, spherical wave model should be considered for accurate signal representation.

The problem of different aspect angles are handled with block-sparse reconstruction in [7]. Block Orthogonal Matching Pursuit (BOMP) is employed to fuse the multi-aspect ISAR images. The same idea is utilized for automotive radar case in [8], where BOMP algorithm is used to optimize the positions of incoherent antenna arrays. However, a better performance in terms of angular resolution is reported with block-FOCUSS algorithm [9].

The state-of-the-art block-FOCUSS method operates with the assumption that different radars observe the targets in the same range bins. This assumption holds for relatively small baseline distances. However, large baseline distance is required for a higher spatial gain. Therefore, in this work, the effect of baseline distance on DoA estimation is investigated. With a larger baseline distance, the difference between measured range values in each radar increases. This leads to a performance degradation in resolution capability. A novel 2D-Localization approach based on block-FOCUSS is proposed to solve this issue. Instead of searching in only angular dimension, range dimension is added into the search grid with the proposed 2D-Localization approach. The performance of the proposed method and the state-of-the-art is illustrated with Monte-Carlo simulations.

The signal model for a distributed radar system is described in Section 2.The non-coherent processing approach with block sparsity is summarized in section 3. In this section, a novel 2D-Localization approach based on Block-FOCUSS is introduced in addition to DoA estimation. Subsequently, the performance of the 2D-Localization method is evaluated in Section 4Finally, the conclusion is given in Section 5.

## 2. Signal Model

A radar network composed of two MIMO radar units are considered in this work as shown in Fig. 1. Each radar unit has an ULA consist of $N$ virtual channels with $\lambda/2$ spacing. The radar units are placed on the x-axis with equal distance from the origin, where this distance creates the baseline $B_l$. The total aperture of a radar network determined by the baseline $B_l$, and the far-field distance is calculated as $2B_l^2/\lambda$. If radar units are widely separated, then the far-field distance of a radar network could reach 500 times of the far-field distance of a single radar unit. However, plane-wave assumption could be still used to define signal model for each radar unit although a target stays in the near-field of the radar network [9]. The key aspect of this formulation is that the radar units observe the same target from different aspect angles as shown in Fig. 1. This leads to change in reflection coefficient observed at each radar unit. Block-sparsity formulation has been proposed to solve this issue [7].

The signal model for the $l^{th}$ radar unit composed of $N$ virtual channels is given by (1). Here, $\mathbf{y}_l \in \mathbb{C}^{N\times 1}$ is the measurement vector which contains samples obtained from $N$ virtual channels after range-Doppler processing. The source vector $\mathbf{x}_l \in \mathbb{C}^{N_s\times 1}$ represents reflection coefficients

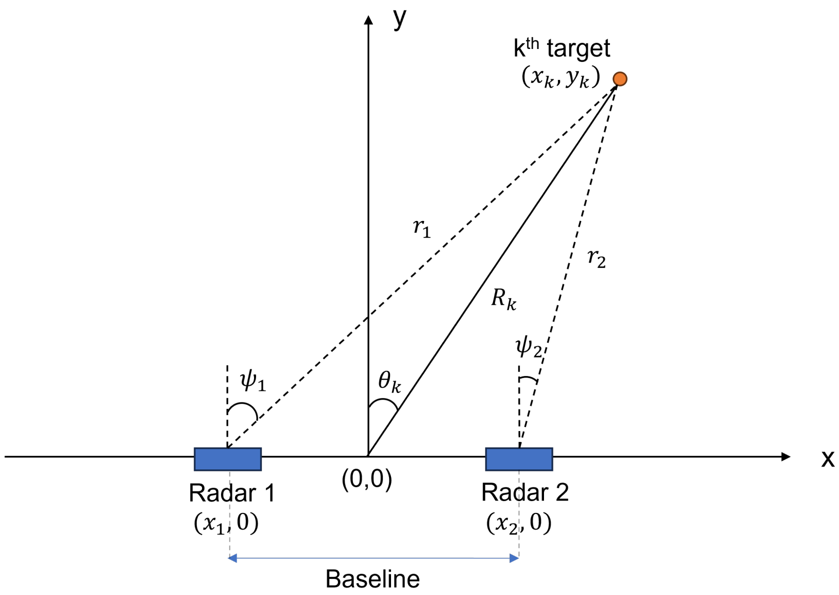


Figure 1: Geometry of a radar network composed of two radar units.

of $N_s$ grid points in the scene. DoA information is described in the sensing matrix $\mathbf{A}_l \in \mathbb{C}^{N \times N_s}$. The sensing matrix $\mathbf{A}_l$ contains different steering vectors for each aspect angle in the defined grid as shown in (2). The additive white Gaussian noise is represented with $\mathbf{n}_l \in \mathbb{C}^{N \times 1}$ in the signal model as:

$$\mathbf{y}_l = \mathbf{A}_l \mathbf{x}_l + \mathbf{n}_l \quad \text{for } l = 1, 2 \tag{1}$$

$$\mathbf{A}_l = \left[\mathbf{a}_l(\theta_1), \mathbf{a}_l(\theta_2), \ldots, \mathbf{a}_l(\theta_{N_s})\right] \text{ where } \mathbf{a}_l(\theta_k) = \left[1, e^{j\frac{2\pi}{\lambda}d\sin(\theta_k)}, \ldots, e^{j\frac{2\pi}{\lambda}(N-1)d\sin(\theta_k)}\right]^T \tag{2}$$

The common grid is defined according to the origin of the radar network for range $R_k$ with $N_s$ points. Different DoA values observed from each radar unit for these grid points are calculated by using geometric relations. The sensing matrices of each radar unit $(\mathbf{A}_l)$ are generated by considering plane-wave assumption, with the calculated DoA values.

In addition to formulation stated in (1), we formulated the same problem with spherical wave model in this work. The first difference in this formulation is that the grid is defined in two-dimensions rather than only angular domain. In this case, the grid points are defined in Cartesian coordinate system with the position vector $\vec{r}_n$, and the source vector $\mathbf{x}_l$ is created by vectorizing the reflection coefficients of $N_s$ grid points. The sensing matrix $\mathbf{A}_l$ takes the form stated in (3). For each grid point, the position vector $\vec{r}_n$ is defined from the origin of the system to the $n^{th}$ grid point.

$$\mathbf{A}_l = \begin{bmatrix} a_1^{(l)}(f_1^{(l)}, \vec{r}_1) & a_1^{(l)}(f_1^{(l)}, \vec{r}_2) & \cdots & a_1^{(l)}(f_1^{(l)}, \vec{r}_{N_s}) \\ \vdots & \vdots & \ddots & \vdots \\ a_1^{(l)}(f_K^{(l)}, \vec{r}_1) & a_1^{(l)}(f_K^{(l)}, \vec{r}_2) & \cdots & a_1^{(l)}(f_K^{(l)}, \vec{r}_{N_s}) \\ a_2^{(l)}(f_1^{(l)}, \vec{r}_1) & a_2^{(l)}(f_1^{(l)}, \vec{r}_2) & \cdots & a_2^{(l)}(f_1^{(l)}, \vec{r}_{N_s}) \\ \vdots & \vdots & \ddots & \vdots \\ a_N^{(l)}(f_K^{(l)}, \vec{r}_1) & a_N^{(l)}(f_K^{(l)}, \vec{r}_2) & \cdots & a_N^{(l)}(f_K^{(l)}, \vec{r}_{N_s}) \end{bmatrix} \quad (3)$$

The elements of $\mathbf{A}_l$ is given for $m^{th}$ channel and $n^{th}$ grid point. Each element of the steering matrix is the product of the point spread function in frequency domain and the propagation delay for the corresponding grid points as given via $a_m^{(l)}(f_k^{(l)}, \vec{r}_n) = P^{(l)}(f_k^{(l)}, \vec{r}_n)\, e^{-j\frac{2\pi}{\lambda}(|\vec{R}_{tx}^{(m)} - \vec{r}_n| + |\vec{R}_{rx}^{(m)} - \vec{r}_n|)}$ The point spread function $P^{(l)}(f_k^{(l)}, \vec{r}_n)$ is defined for $K$ frequency points where $f_k^{(l)}$ are the discrete frequency bins for the $l^{th}$ radar unit. For an FMCW radar, point spread function $P^{(l)}(f_k^{(l)}, \vec{r}_n)$ after range-Doppler processing would be equivalent to the beat spectrum. Besides point spread function, the propagation delay is calculated for the $m^{th}$ MIMO channel between the transmitter at $\vec{R}_{tx}^{(m)}$ and the receiver at $\vec{R}_{rx}^{(m)}$. This leads to the second difference in the formulation, where the spherical wave model is considered.

# 3. Non-Coherent Processing for a Radar Network

## 3.1. Block-FOCUSS Algorithm

Block-FOCUSS algorithm is an extension of FOCUSS algorithm with block-sparsity assumption. It is assumed that the source vector $\mathbf{x}_l$ observed from each radar unit has the non-zero values at the same position. Block-sparsity is formulated with $\ell_{2,1}$ norm in the optimization problem as given in (4) [9]. Here, $\mathbf{X}$ matrix is created by stacking every source vector $\mathbf{x}_l$ from $L$ radar units. $\ell_{2,1}$ norm is calculated in two steps. Firstly, $c_n$ values are calculated which is the $\ell_2$-norm of each row of $\mathbf{X}$ matrix. In the second step, $\ell_1$-norm of $c_n$ values are calculated to achieve $\ell_{2,1}$ norm of $\mathbf{X}$ matrix. For $L$ number of radar units, the details of Block-FOCUSS algorithm are described in Algorithm 1. When this algorithm is utilized for DoA estimation, the sensing matrices $\mathbf{A}_l$ stated in (2) are formed as described in [9].

$$\min_{\mathbf{x}_1,\ldots,\mathbf{x}_L} \sum_{l=1}^{L} \|\mathbf{y}_l - \mathbf{A}_l\mathbf{x}_l\|_2^2 + \mu\|\mathbf{X}\|_{2,1} \quad (4)$$

## 3.2. Proposed 2D-Localization Approach based on Block-FOCUSS

In this work, we proposed a 2D-Localization approach based on Block-FOCUSS. Different from DoA estimation with Block-FOCUSS, the search grid is defined in two dimensions. This

**Algorithm 1** Block FOCUSS algorithm for multiple apertures

Inputs: $\mathbf{y}_l,\ \mathbf{A}_l$ for $l = [1, 2, \dots, L]$
Outputs: $\hat{\mathbf{x}},\ \delta$
Initialize $k = 0;\ \mathbf{W}^{(0)} = \mathbf{I};\ \delta_t = 10^{-8};\ \delta = 1;\ \hat{\mathbf{x}}^{(0)} = \mathbf{y};\ \mu =$ noise variance
**while** $\delta > \delta_t$ **do**
    $k = k + 1$
    **for** $l = [1, 2, \dots, L]$ **do**
        $\mathbf{A}_l^{(k)} = \mathbf{A}_l \mathbf{W}^{(k-1)}$
        $\mathbf{q}_l^{(k)} = (\mathbf{A}_l^{(k)})^H \left( \mathbf{A}_l^{(k)} (\mathbf{A}_l^{(k)})^H + \mu \mathbf{I} \right)^{-1} \mathbf{y}_l$
        $\mathbf{x}_l^{(k)} = \mathbf{W}^{(k-1)} \mathbf{q}_l^{(k)}$
    **end for**
    $\mathbf{X} = \begin{bmatrix} \mathbf{x}_1 & \mathbf{x}_2 & \dots & \mathbf{x}_L \end{bmatrix} \in \mathbb{C}^{N_s x L}$
    $\|\mathbf{X}\|_{2,p} = \sum_{n=1}^{N_s} (c_n)^p$ where $c_n = \sqrt{\sum_{l=1}^{L} |x_{n,l}|^2}$
    $\mathbf{W}^{(k)} = \operatorname{diag}\left( (c_1^{(k)})^p, (c_2^{(k)})^p, \dots, (c_{N_s}^{(k)})^p \right)$
    $\hat{\mathbf{x}} = \left[ (c_1^{(k)})^p, (c_2^{(k)})^p, \dots, (c_{N_s}^{(k)})^p \right]^T$
    $\delta = \frac{\|\hat{\mathbf{x}}^{(k)} - \hat{\mathbf{x}}^{(k-1)}\|_2}{\|\hat{\mathbf{x}}^{(k-1)}\|_2}$
**end while**

leads to an increase in the computational cost because the search grid becomes bigger. Therefore, two steps are applied to decrease the dimension of the sensing matrices $\mathbf{A}_l$ before utilizing them in Block-FOCUSS algorithm. The first step is to select a region of interest. The coarse angular estimation from single radar units is utilized to determine the region of interest. Instead of scanning a large area, the algorithm only looks for a region where at least one target presents. The second step is that only three frequency points of the beat spectrum is employed for point spread function $P^{(l)}(f_k^{(l)}, \vec{r}_n)$. The detected beat frequency and the adjacent bins are involved into the sensing matrix. All steps applied in 2D-Localization approach are listed in Algorithm 2.

**Algorithm 2** 2D-Localization Approach based on Block-FOCUSS

Obtain range-angle estimation for each radar unit
Determine region of interest for search grid
Generate sensing matrices $\mathbf{A}_l$'s as given in (3)
Apply Block-FOCUSS algorithm given in Algorithm 1 with the generated sensing matrices

Various grid definitions could be employed to define a search grid in two dimensions. In this work, two different grid definitions are investigated based on Cartesian coordinates and polar coordinates. For both grid definitions, the origin is the same as the origin of the radar network. Examples for both grid definitions are illustrated in Fig. 2. The performance obtained with two grid definitions are compared in the results section.

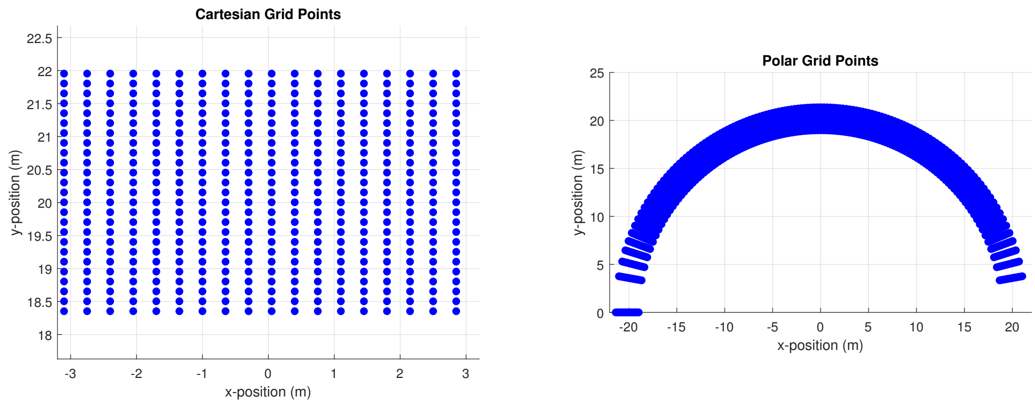


(a) Search grid with Cartesian coordinates (b) Search grid with polar coordinates

Figure 2: Example search grid points for 2D-Localization method.

## 4. Simulation Results

Monte-Carlo (MC) simulations are conducted to evaluate the performance of the described methods in this work. A radar network composed of two identical MIMO radars is employed in the simulations. The parameters of a single radar unit is given in Table 1. The baseline distance is changed from $0.5$ m to $3$ m by $0.5$ m steps. For $0.5$ m baseline distance, the far-field distance is calculated as $125$ m. The targets are located at $20$ m range. Therefore, the simulated targets stay in the near-field of the system.

Table 1: Radar parameters used in MC simulations

| Parameter | Values |
|---|---|
| Center frequency | 78.0 GHz |
| Bandwidth (B) | 250 MHz |
| Sweep Time (T) | 25.6 $\mu$s |
| Number of chirps | 16 |
| Sampling frequency | 10 MHz |
| Number of transmitters | 3 |
| Number of receivers | 4 |

Angular resolution capability of the discussed methods in near field is evaluated by Monte Carlo simulations. Two point targets are placed at $20$ m range, and the angular separation of the targets varies between $1°$ to $10°$ with $1°$ steps. The test targets are located between $-30°$ to $30°$. In each MC simulation, target phase is realized with $U(0, 2\pi)$. SNR value is 20 dB after range-Doppler processing. The performance is assessed via running 500 signal realizations for each angular separation case. DoA estimation performance is evaluated by three metrics: probability of resolution (PR), root-mean-square-error (RMSE), and the false alarm rate (FAR).

The effect of baseline distance on the performance of DoA estimation is investigated with the described MC dataset. DoA estimation with block-FOCUSS and B-OMP are compared with the proposed 2D-Localization approach. When the baseline distance is 1 m, the resolution capability of different methods are illustrated in Fig. 3(a). Compared to block-FOCUSS based approaches, BOMP is not capable of resolving targets that are separated by less than the angular resolution of a single radar. Among block-FOCUSS based methods, 2D-Localization approach using polar grid performs similarly to DoA estimation with block-FOCUSS. However, employing a Cartesian grid does not offer any advantage. Instead, it results in lower PR and higher RMSE. FAR is even higher than that observed with BOMP.

The performance metrics for varying baseline distances ranging from 0.5 m to 3 m are presented in Fig. 3(b). The reported values represent the mean performance across all angular separation scenarios for each baseline distance. The different methods exhibit similar behavior to that observed in Fig. 3(a). However, for block-FOCUSS based methods, a decline in PR metric and an increase in RMSE is observed as the baseline distance increases. This performance degradation occurs due to the violation of the assumption made in [9], which requires that both radars observe the targets within the same range bin. When the baseline distance exceeds 2 m, this condition no longer holds, and the block-FOCUSS algorithm receives measurements from only one radar. However, the methods maintain high resolution capability due to the inherent performance characteristics of FOCUSS algorithm.

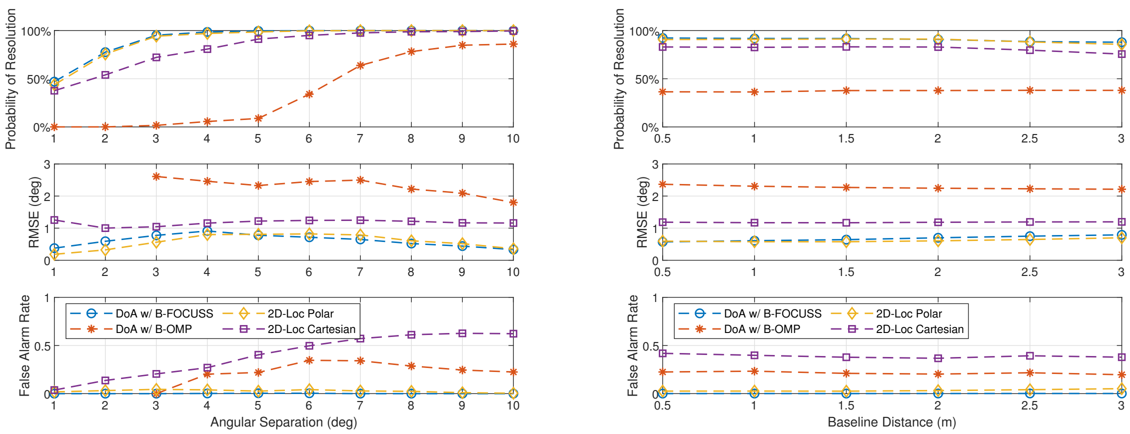


(a) (b)

Figure 3: (a) Comparison of performance metrics for different methods when the baseline distance is 1 m. (b) Effect of baseline distance on the performance metrics.

## 5. Conclusion

Radar networks are utilized to overcome low angular resolution of simple MIMO radars due to the limited size of their apertures. For non-coherent processing methods, block-FOCUSS and BOMP algorithms are two of the state-of-the-art approaches. These methods rely on the assumption that the radars observe the targets in the same range bin. However, this assumption is no longer satisfied as the baseline distance increases. In this work, the effect of baseline distance on DoA estimation performance is investigated. Besides the state-of-the-art methods, a novel 2D-Localization approach based on block-FOCUSS is proposed. Two different grid definitions are chosen as Cartesian grid and polar grid. When the resolution capability of the state-of-the-art and the proposed methods are compared, a performance degradation is observed with larger baseline distances. A similar behavior to DoA estimation with block-FOCUSS is obtained with the proposed 2D-Localization approach. Future work will focus on investigating potential performance improvements of 2D-Localization approach.

## References


[1] G. Hakobyan and B. Yang, “High-Performance Automotive Radar: A Review of Signal Processing Algorithms and Modulation Schemes”, *IEEE Signal Processing Magazine*, vol. 36, no. 5, pp. 32-44, Sept. 2019.

[2] C. Waldschmidt, J. Hasch and W. Menzel, “Automotive Radar — From First Efforts to Future Systems”, *IEEE Journal of Microwaves*, vol. 1, no. 1, pp. 135-148, Jan. 2021.

[3] M. Gottinger et al., “Coherent Automotive Radar Networks: The Next Generation of Radar-Based Imaging and Mapping”, *IEEE Journal of Microwaves*, vol. 1, no. 1, pp. 149-163, Jan. 2021.

[4] C. Buchberger, A. Schoisl, O. Kepenek and E. Biebl, “Equivalent Angular Resolution for Distributed Radar Sensors”, *2022 Asia-Pacific Microwave Conference (APMC)*, Yokohama, Japan, 2022.

[5] A. Pirkani, D. Kumar, M. Cherniakov and M. Gashinova, “Distributed Automotive Radar Multi-Modal Sensing”, *2023 20th European Radar Conference (EuRAD)*, Berlin, Germany, 2023, pp. 319-322.

[6] A. Dürr, B. Schneele, D. Schwarz and C. Waldschmidt, “Range-Angle Coupling and Near-Field Effects of Very Large Arrays in mm-Wave Imaging Radars”, *IEEE Transactions on Microwave Theory and Techniques*, vol. 69, no. 1, pp. 262-270, Jan. 2021.

[7] S. Brisken and J. Ender, “Block-sparse 3-D ISAR image reconstruction in a non-coherent multi-static scenario”, *2015 IEEE Radar Conference (RadarCon)*, Arlington, VA, USA, May 2015, pp. 0265–0269.

[8] D. Mateos-Núñez, R. Simoni, M. A. González-Huici and A. Correas-Serrano, “Design of mutually incoherent arrays for DoA estimation via group-sparse reconstruction”, *2019 IEEE Radar Conference (RadarConf)*, Boston, MA, USA, April 2019, pp. 1–6.

[9] A. R. Suvarna, A. Koppelaar, F. Jansen, J. Wang and A. Yarovoy, “Fusion of Data from Multiple Automotive Radars for High-Resolution DoA Estimation”, *2022 IEEE Radar Conference (RadarConf22)*, New York City, NY, USA, March 2022, pp. 1–5.